

FAME: Fairness-aware Attention-modulated Video Editing

Zhangkai Wu¹, Xuhui Fan¹, Zhongyuan Xie¹, Kaize Shi², Zhidong Li³, Longbing Cao¹

¹ Macquarie University, Australia

² University of Southern Queensland, Australia

³ University of Technology Sydney, Australia

Abstract

Training-free video editing (VE) models tend to fall back on gender stereotypes when rendering profession-related prompts. We propose **FAME** for *Fairness-aware Attention-modulated Video Editing* that mitigates profession-related gender biases while preserving prompt alignment and temporal consistency for coherent VE. We derive fairness embeddings from existing minority representations by softly injecting debiasing tokens into the text encoder. Simultaneously, FAME integrates fairness modulation into both temporal self attention and prompt-to-region cross attention to mitigate the motion corruption and temporal inconsistency caused by directly introducing fairness cues. For temporal self attention, FAME introduces a region constrained attention mask combined with time decay weighting, which enhances intra-region coherence while suppressing irrelevant inter-region interactions. For cross attention, it reweights tokens to region matching scores by incorporating fairness sensitive similarity masks derived from debiasing prompt embeddings. Together, these modulations keep fairness-sensitive semantics tied to the right visual regions and prevent temporal drift across frames. Extensive experiments on new VE fairness-oriented benchmark *FairVE* demonstrate that FAME achieves stronger fairness alignment and semantic fidelity, surpassing existing VE baselines.

1 Introduction

Video editing with text prompts has witnessed rapid development thanks to the rise of text-to-image (T2I) Diffusion Models (DM) such as Stable Diffusion (SD) (Rombach et al. 2022) and DALLE-E (Ramesh et al. 2021). Building upon these pre-trained T2I models, recent training-free VE methods (Qi et al. 2023; Geyer et al. 2024; Liu et al. 2024b; Yang et al. 2025) enable flexible control over object appearance, motion, and semantics, by manipulating temporal self-attention and cross-frame attention maps.

On the other hand, generating fair content from pre-trained vision-language models has become an increasingly critical problem. (Cho, Zala, and Bansal 2023) first revealed that T2I models often reproduce gender and racial stereotypes, even for given neutral prompts (Cho, Zala, and Bansal 2023; Shen et al. 2024; Gandikota et al. 2024). This *social bias* largely stems from imbalanced image-text pairs, where data associated with perpetuate majority groups is more frequently collected, and from inherent biases in large-scale

language models used in text encoders such as CLIP (Ross, Katz, and Barbu 2021; Birhane, Prabhu, and Kahembwe 2021). However, existing fairness-aware T2I methods (Li et al. 2024a; Kim et al. 2025) focus on static images only, which often rely on prompt-image alignment assumptions that may not be generalized to temporally coherent video generation.

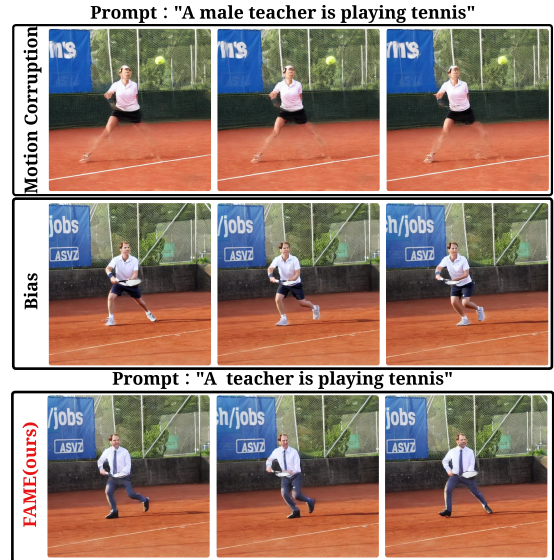


Figure 1: Training-free VE methods (e.g., TokenFlow (Geyer et al. 2024)) fail to correct gender stereotypes in profession related prompts, as shown in the 1st row, even with debiasing prompt, causing motion corruption, with missing actions, ghosting, and temporal discontinuity. Videograin (Yang et al. 2025) partly reduces bias but still retains stereotypical features such as outfit, illustrated in the 2nd row. In contrast, FAME combines soft prompt encoding and attention modulation to remove both profession bias and motion corruption, generating coherent videos with accurate debiased profession details.

Bridging these two lines of research reveals a significant gap: *fairness-aware VE in a training-free setting has not been formally explored*. Existing T2I models exhibit gen-

der bias toward profession related prompts, defaulting to stereotypical gender content. When debiasing prompts are applied, these models often suffer from motion corruption, manifesting as semantic mismatch, visual inconsistency, and degraded controllability. More details are revealed in Figure 1 and our Prompt Responsiveness Test in Appendix Figure 5. These observations highlight the need for a dedicated framework that can achieve fairness control without compromising motion consistency.

To bring fairness into VE while still preserving prompt meaning and motion quality, **FAME** (Fairness-aware Attention-modulated VE) as a training-free approach tackles both bias and motion corruption together. To reduce gender bias in profession related prompts while preserving their original meaning, we introduce *soft debiasing prompt encoding*, which gently adjusts prompt embeddings toward fairness-aware semantics without altering the intended content. Yet debiasing at the prompt level alone cannot stop fairness cues from fading over time, so we add *temporal self-attention modulation* to maintain fairness consistency across frames and avoid temporal attention dilution. Finally, since fairness tokens can still drift from their correct visual regions during denoising, we apply *cross-attention reweighting* to better align fairness related prompts with the corresponding spatial regions.

On open source benchmarks, FAME consistently outperforms state-of-the-art training-free VE models in fairness preservation, semantic accuracy, and visual consistency, as measured by both CLIP based metrics and human evaluations. Our main contributions are summarized as follows:

- **FairVE**, as the first benchmark that exploits existing open source datasets and protocols to evaluate fairness in T2I based VE models.
- **FAME**, as a training-free framework to jointly mitigate bias and motion corruption through prompt encoding, temporal attention modulation, and cross attention reweighting at the inference time.
- The **state-of-the-art** performance in fairness preservation, semantic alignment, and temporal coherence by FAME.

2 Video Editing Models and Fairness

Video Editing Models

Latent diffusion models are commonly used, which first encode the input image sequence \mathcal{X} into a latent representation \mathbf{z}_0 and then gradually corrupt \mathbf{z}_0 through a forward diffusion process, resulting in intermediate latent variables $\{\mathbf{z}_t\}_t$ and their associated attention maps.

$$q(\mathbf{z}_t | \mathbf{z}_{t-1}) = \mathcal{N}\left(\mathbf{z}_t; \sqrt{1 - \beta_t} \mathbf{z}_{t-1}, \beta_t \mathbf{I}\right),$$

where $t = 1, \dots, T$, with T denoting the total number of steps in the forward diffusion process. The parameter β_t controls the noise strength injected at timestep t . After defining the forward process, a backward inversion process is used to denoise the noise data into original data, with each step defined as:

$$p_{\theta}(\mathbf{z}_{t-1} | \mathbf{z}_t) = \mathcal{N}\left(\mathbf{z}_{t-1}; \boldsymbol{\mu}_{\theta}(\mathbf{z}_t, t), \sigma_t^2 \mathbf{I}\right),$$

where $\boldsymbol{\mu}_{\theta}(\mathbf{z}_t, t)$ denotes the prediction of \mathbf{x}_0 at step t , and σ_t^2 is the variance in the inverse step. In practice, the notable U-Net architecture is usually involved in designing the neural architecture of $\boldsymbol{\mu}_{\theta}(\mathbf{z}_t, t)$. Further, linear transformed denoising model $\epsilon_{\theta}(\mathbf{z}_t, t)$ is usually used to predict the residual noise, replacing $\boldsymbol{\mu}_{\theta}(\mathbf{z}_t, t)$ for computational convenience as:

$$\mathbf{z}_{t-1} = \sqrt{\frac{\alpha_{t-1}}{\alpha_t}} \mathbf{z}_t + \left(\sqrt{\frac{1 - \alpha_{t-1}}{\alpha_{t-1}}} - \sqrt{\frac{1 - \alpha_t}{\alpha_t}} \right) \epsilon_{\theta}(\mathbf{z}_t, t),$$

where $\alpha_t = 1 - \beta_t$ defines the retention ratio of signal. Classifier-free methods (Ho and Salimans 2022) have become a mainstream approach for T2I generation, with the residual noise model $\epsilon_{\theta}(\mathbf{z}_t, t)$ modified as:

$$\tilde{\epsilon}_{\theta}(\mathbf{z}_t, t, \phi(\mathbf{p}_{\text{ref}}), \emptyset) = w \cdot \epsilon_{\theta}(\mathbf{z}_t, t, \phi(\mathbf{p}_{\text{ref}})) + (1 - w) \cdot \epsilon_{\theta}(\mathbf{z}_t, t, \emptyset), \quad (1)$$

where $\phi(\cdot)$ is the text encoder. The combined noise prediction $\tilde{\epsilon}_{\theta}$ is obtained by linearly interpolating between the conditional prediction (conditioned on the prompt) and the unconditional prediction, with a weighting factor $w \in [0, 1]$ by null-text optimization trick (Ho and Salimans 2022; Mokady et al. 2023).

In training-free VE models, attention maps in the residual noise model $\epsilon_{\theta}(\mathbf{z}_t, t, \phi(\mathbf{p}_{\text{ref}}), \emptyset)$ are extracted during the inversion stage to preserve the spatio-temporal consistency across frames. In detail, these models replace the reference prompt \mathbf{p}_{ref} with target prompt \mathbf{p}_{tar} to predict the noise component $\epsilon_{\theta}(\mathbf{z}_t, t, \phi(\mathbf{p}_{\text{tar}}))$ via the following reverse process:

$$\tilde{\epsilon}_{\theta}(\mathbf{z}_t, t, \phi(\mathbf{p}_{\text{tar}}), \emptyset) = w \cdot \epsilon_{\theta}(\mathbf{z}_t, t, \phi(\mathbf{p}_{\text{tar}})) + (1 - w) \cdot \epsilon_{\theta}(\mathbf{z}_t, t, \emptyset). \quad (2)$$

This guidance mechanism enables controllable generation aligned with textual editing intents while maintaining temporal coherence in video frames.

Fairness in Video Editing

T2I-Based VE Models Due to the high inference cost of text-to-video (T2V) models (Ho et al. 2022; Singer et al. 2022; Wu et al. 2023a) and the scarcity of high-quality video-text pairs, many recent methods adopt open-source T2I frameworks (Rombach et al. 2022) to enable VE guided by user-provided text or visual cues. Tune-A-Video (TAV) (Wu et al. 2023b) fine-tunes a LoRA module that embeds temporal features to support multi-frame inputs, enabling high-quality and controllable VE. Leveraging the scalability of pre-trained LoRA modules, TAV-based approaches advance the integration of visual components into the base model. For example, CCEdit (Feng et al. 2024) introduces two distinct injection networks to control appearance and structure separately. CAMEL (Zhang et al. 2024) employs CLIP-based prompt embeddings to enhance motion consistency across frames, thereby improving alignment with user intent. DeCo (Zhong et al. 2025) incorporates a NeRF-based module to improve the 3D perception of human subjects.

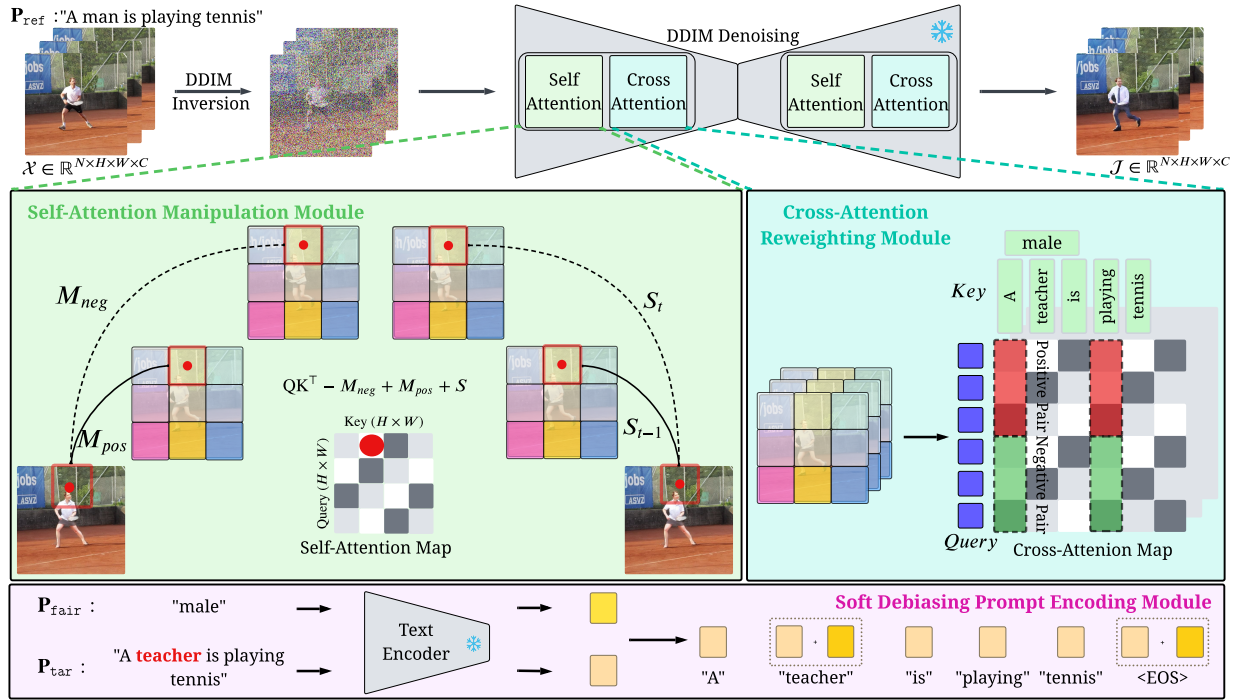


Figure 2: Framework of FAME. In the denoising process, the soft debiasing prompt encoding module will encode the debiasing prompt P_{tar} explicitly and fuse the self-attention map QK^T with time decay S and element weight M with cross-attention map reweighting.

Training-free T2I-Based VE Models While TAV-based methods incorporate additional trainable components, training-free approaches offer advantages such as faster inference and lower resource consumption. FateZero (Qi et al. 2023) introduces cross-frame attention modules to extract spatio-temporal attention maps, guiding multi-frame generation based on prompt variations. Focusing on the training-free pipeline itself, methods such as STEM (Li et al. 2024b), WAVE (Feng et al. 2025), SliceEdit (Cohen et al. 2024), and COVE (Wang et al. 2024) refine the video inversion stage by selecting key frames to ensure temporal consistency. TokenFlow (Geyer et al. 2024) and Vid2Me (Li et al. 2024c) focus on designing spatio-temporal attention maps to enhance prompt consistency during generation. Another line of work integrates external T2I plugins for fine-grained image to VE frames control. For instance, Ground-A-Video (Jeong and Ye 2024), RAVE (Kara et al. 2024), and VideoShop (Fan, Bhattad, and Krishna 2024) adopt ControlNet variants, while OCD (Kahatapitiya et al. 2025) and VideoGrain (Yang et al. 2025) leverage the Segment Anything Model to enable object-aware VE. Despite substantial progress in editing quality and task diversity, fairness issues in VE remain largely unaddressed.

Fair T2I Generation Models. To suppress *social bias* in T2I model generated content, semantic debiasing methods introduce predefined corrective semantic concepts, which are learned either by optimizing the diffusion model in applying classifier-guidance techniques (Brack et al. 2023; Dewan et al. 2024; Shen et al. 2024; Jung et al. 2025),

or gradient based modules (Huang et al. 2025; Azam and Akhtar 2025; Li et al. 2025c; Lee, Lim, and Chun 2025) to adjust the noise predictor or directly modifying the text prompt embedding space (Kim et al. 2025). However, finetuning the entire SD model is computationally expensive, as it requires retraining a large number of parameters. Cross-attention map debiasing approaches (Gandikota et al. 2024; Teo et al. 2024; Zhou et al. 2024; Jung, Jang, and Wang 2024; Park et al. 2025) aim to mitigate stereotypical prototypes encoded within the key–query alignment space. In parallel, feature-level debiasing methods (Li et al. 2024a; Shi et al. 2025) seek to learn fairness-aware embeddings by modulating the intermediate representations within the U-Net bottleneck. Despite notable advances in image generation, fairness concerns in T2I-based VE models remain largely underexplored.

3 Methodology

Prompt Responsiveness Test for Fairness Verification in Video Editing

Although various T2I-based debiasing methods (Shen et al. 2024; Gandikota et al. 2024; Kim et al. 2025) have demonstrated that debiasing regions in the latent space of SD variants can be effectively explored, either through classifier-free guidance to embed fair content or by incorporating priors into pre-trained model components, it still remains unclear whether such fairness-guided mechanisms remain effective when extended to VE models. For instance, in recent

training-free VE models, cross frame attention mechanisms are introduced to ensure temporal consistency, which fundamentally alters the original prompt semantic coherence, i.e., the alignment between prompt semantics and visual features that underlies T2I models.

As a result, directly transferring fairness control strategies from T2I to VE remains a challenging and open research problem. To assess whether training-free VE models still preserve debiasing regions, we propose the *Prompt Responsiveness Test* designed to evaluate the model’s ability to respond to explicitly debiasing textual conditions.

Prompt Responsiveness Test To assess whether VE models can preserve fairness-related cues in textual prompts, the prompt responsiveness test can be implemented by incorporating a gender-specific hint with the original professions (e.g., $\mathbf{P}_{\text{tar}} = \text{"a male teacher is playing tennis"}$) directly into the target editing prompt. These gender-profession prompt templates are adapted from prior work (Kim et al. 2025). We then examine whether the generated videos visually reflect the intended gender identity, and whether the direct use of debiasing prompts affects the editing performance.

We apply this test in several training-free VE models. The resulted video (line 2-4 in Appendix Figure 5) fails to align with the prompt, when gender is explicitly specified in the prompt. This misalignment may be traced back to the introduction of cross-frame attention and latent feature fusion. That is, directly transferring T2I’s prompt-based fairness control to VE might not work. An alignment-aware debiasing strategy is required for the fairness VE. More details and visualized results can be referred to the Appendix Figure 5.

The Training-free FAME Model

We observe three key challenges when extending fairness-aware image editing methods to VE: (1) directly injecting debiasing prompts may disrupt the semantic structure of generated content; (2) fairness-aware local features tend to be diluted by global feature fusion, especially over temporal sequences; and (3) prompt-to-region attention may become inconsistently distributed across frames.

Addressing these challenges, we introduce FAME, a training-free VE framework that incorporates fairness into generation through three key components: (1) the *soft debiasing prompt encoding* module, which injects fairness intent into prompts with minimal semantic disruption; (2) the *temporal self-attention modulation* module, which preserves intra-region coherence across frames; and (3) the *cross-attention reweighting* module, which improves alignment between fairness-sensitive tokens and visual regions. All modules are operated at the inference time and no model retraining is required.

Overall Framework. Given an input video $\mathcal{X} = \{\mathbf{X}^1, \mathbf{X}^2, \dots, \mathbf{X}^N\}$, where each frame $\mathbf{X}^n \in \mathbb{R}^{H \times W \times C}$ and the N , H , W , and C denote the frame number, height, width, and channel dimensions, respectively, we consider a fairness-aware VE task guided by a composite textual prompt. This prompt comprises a reference prompt \mathbf{p}_{ref} (e.g., "A man is playing tennis."), a target prompt \mathbf{p}_{tar} (e.g., "A teacher is playing

tennis."), and a debiasing attribute indicator \mathbf{p}_{fair} (e.g., "Male"), which specifies the direction of bias to be corrected. The objective is to generate an edited video $\mathcal{J} = \{J^1, \dots, J^N\}$, where each frame $J^n \in \mathbb{R}^{H \times W \times C}$ reflects the intent of the edited prompt, while maintaining temporal consistency across frames and alignment with fairness constraints. The whole pipeline is illustrated in Figure 2.

The proposed FAME is a fairness-aware VE framework that integrates prompt debiasing and attention modulation. First, we define a fair attribute embedding function $g(\mathbf{p}_{\text{tar}}, \mathbf{p}_{\text{fair}})$ that encodes a selected subset of fairness-sensitive prompt tokens into embeddings for debiasing target text. Each \mathbf{p}_{fair} is encoded using an SD text encoder. Second, leveraging the fairness-aware text embedding’s attention maps during the inversion stage, we introduce two functions: self-attention manipulation function $f(\cdot)$ and cross-attention reweighting function $h(\cdot)$, to produce a region-wise attention maps $\{\mathbf{a}_k\}_k \in [0, 1]^{H \times W}$. Each entry $a_{k,hw}$ denotes the spatial attention mask value of the k -th region relevant to the w -th fairness attribute.

As a result, the process of VE can be described by a model $\mathcal{M}(g, f, h; \mathbf{p}_{\text{ref}}, \mathbf{p}_{\text{tar}}, \mathbf{p}_{\text{fair}})$, wherein $f(\cdot)$ and $h(\cdot)$ jointly modulate spatio-temporal attention during inference to produce the final edited video \mathcal{J} in alignment with the intended fairness objective.

Soft Debiasing Prompt Encoding for Fairness Preservation.

Given a fairness attribute prompt \mathbf{p}_{fair} (e.g., "female" or "male"), the CLIP-based text encoder $\phi(\cdot)$ produces the token embeddings $\mathbf{e}_{\text{fair}} = \phi(\mathbf{p}_{\text{fair}}) \in \mathbb{R}^{l_1 \times d}$ from \mathbf{p}_{fair} , where l_1 is the number of tokens and d is the embedding dimension. Similarly, the target prompt \mathbf{p}_{tar} ’s token embedding is obtained as $\mathbf{e}_{\text{tar}} = \phi(\mathbf{p}_{\text{tar}}) \in \mathbb{R}^{l_2 \times d}$. The soft debiasing prompt encoding may be proceeded in two steps without requiring additional training or architectural modifications.

In the first step, we identify a set of token positions $\mathcal{P} \subseteq \{1, \dots, l_2\}$ in \mathbf{p}_{tar} that are semantically relevant to fairness and softly fuse their embeddings with the corresponding fairness tokens:

$$\tilde{\mathbf{e}}_k = \lambda_k \cdot \mathbf{e}_{\text{tar},k} + (1 - \lambda_k) \cdot \mathbf{e}_{\text{fair},k}, \quad \text{for } k \in \mathcal{P}, \quad (3)$$

where $\lambda_k \in [0, 1]$ is a mixing coefficient, either fixed (e.g., 0.5) or derived from attention-based importance scores. Tokens outside \mathcal{P} remain unchanged, resulting in an intermediate embedding matrix $\tilde{\mathbf{e}}_{\text{tar}} \in \mathbb{R}^{l_2 \times d}$.

In the second step, we further refine the debiasing effect by replacing the End of Sequence (EOS) token embedding in $\tilde{\mathbf{e}}_{\text{tar}}$ with the corresponding token from \mathbf{e}_{fair} . This is implemented via a binary injection mask $\mathbf{M} \in \{0, 1\}^{l_2 \times d}$ that activates only at the EOS position by fair attribute embedding function $g(\cdot)$:

$$g(\mathbf{p}_{\text{tar}}, \mathbf{p}_{\text{fair}}) = \tilde{\mathbf{e}}_{\text{tar}} + \mathbf{M} \otimes (\mathbf{e}_{\text{fair}} - \tilde{\mathbf{e}}_{\text{tar}}), \quad (4)$$

where the subtraction and injection are applied only at the EOS token location, since the EOS token in diffusion text encoders aggregates global prompt semantics, allowing fairness information to be injected without disrupting local word-level alignments.

This two-step fusion strategy allows fairness cues to be softly injected into semantically meaningful regions while explicitly guiding the global prompt embedding via EOS-level replacement. Compared to static prompt editing, our method enables more interpretable and localized debiasing, preserving the semantics of original prompt and reducing latent space drift.

Enhancing Intra-region Coherence in Temporal Self-Attention. To enforce temporal coherence within fairness-sensitive regions, we enhance the temporal self-attention mechanism in the latent space by selectively amplifying intra-region attention while suppressing inter-region interference. Given an input latent tensor $\mathbf{z}_t \in \mathbb{R}^{h \times w \times \ell \times c}$, we reshape it with a temporal attention preparation function φ :

$$\varphi: \mathbb{R}^{h \times w \times \ell \times c} \rightarrow \mathbb{R}^{(h \cdot w) \times \ell \times c}, \quad (5)$$

which flattens the spatial dimensions and aligns features along the temporal axis. The resulting features are projected into query, key, and value matrices:

$$\mathbf{Q} = W_{\mathbf{Q}} \cdot \varphi(\mathbf{z}_t), \quad \mathbf{K} = W_{\mathbf{K}} \cdot \varphi(\mathbf{z}_t), \quad \mathbf{V} = W_{\mathbf{V}} \cdot \varphi(\mathbf{z}_t), \quad (6)$$

where $W_{\mathbf{Q}}, W_{\mathbf{K}}, W_{\mathbf{V}} \in \mathbb{R}^{c \times d}$ are learnable matrices.

Inspired by self-attention fusion methods (Chefer et al. 2024; Liu et al. 2024a; Karmann and Urfalioglu 2025), we define the fairness-aware self-attention operator with self-attention manipulation function $f(\cdot)$ as:

$$\text{FairAttention}(\mathbf{Q}, \mathbf{K}, \mathbf{V}) = \text{softmax}(f(\mathbf{Q}, \mathbf{K})) \cdot \mathbf{V}, \quad (7)$$

which incorporates fairness-aware modulation and structural guidance:

$$f(\mathbf{Q}, \mathbf{K}) = \frac{\mathbf{Q}\mathbf{K}^{\top} + \lambda\mathbf{M}^{\text{fair}} + \mu\mathbf{S}}{\sqrt{d}}, \quad (8)$$

where λ and μ are modulation coefficients, and \mathbf{M}^{fair} is defined as

$$\mathbf{M}^{\text{fair}} = \mathbf{R} \odot \mathbf{M}^{\text{pos}} - (1 - \mathbf{R}) \odot \mathbf{M}^{\text{neg}}, \quad (9)$$

with positive and negative maps computed as:

$$\begin{aligned} \mathbf{M}^{\text{pos}} &= \max(\mathbf{Q}\mathbf{K}^{\top}) - \mathbf{Q}\mathbf{K}^{\top}, \\ \mathbf{M}^{\text{neg}} &= \mathbf{Q}\mathbf{K}^{\top} - \min(\mathbf{Q}\mathbf{K}^{\top}), \end{aligned} \quad (10)$$

respectively, and the binary region indicator \mathbf{R} is defined element-wise as:

$$\mathbf{R}[x, y] = \begin{cases} 1, & \text{if } \text{region_id}(x) = \text{region_id}(y), \\ 0, & \text{otherwise.} \end{cases} \quad (11)$$

Here, \mathbf{M}^{fair} modulates attention logits by reinforcing similarities within the same fairness-sensitive region (via \mathbf{M}^{pos}) and weakening correlations across different regions (via \mathbf{M}^{neg}). The binary mask \mathbf{R} simply acts as a selector: it is 1 when two tokens belong to the same region and 0 otherwise, enabling region-specific adjustment.

To further provide region-aware flexibility, we define a soft similarity mask $\mathbf{S} \in \mathbb{R}^{(h \cdot w) \times (h \cdot w)}$ based on temporal feature statistics:

$$\mathbf{S}[\mathfrak{q}_1, \mathfrak{q}_2] = \exp\left(-\frac{\|\mathbf{f}_{\mathfrak{q}_1} - \mathbf{f}_{\mathfrak{q}_2}\|^2}{\tau^2}\right), \quad (12)$$

where each $\mathbf{f}_{\mathfrak{q}}$ is the mean feature vector at spatial position \mathfrak{q} across ℓ frames $\mathbf{f}_{\mathfrak{q}} = \frac{1}{\ell} \sum_{t=1}^{\ell} \mathbf{z}_t[\mathfrak{q}]$, and τ controls the sharpness of the similarity response. The soft mask \mathbf{S} enables continuous region-aware attention modulation, providing a fairness-aligned bias signal complementary to the discrete mask \mathbf{R} .

Prompt-to-Region Alignment Across Frames To enhance alignment between fairness-related textual concepts and visual regions across frames, we propose a fairness-aware cross-attention modulation strategy that adjusts attention scores during the denoising process in the latent space.

Specifically, we define a fairness-aware cross-attention operator with cross-attention reweighting function $h(\cdot)$:

$$\text{FairCrosAttn}(\mathbf{Q}_t, \mathbf{K}_t, \mathbf{V}_t) = \text{softmax}(h(\mathbf{Q}_t, \mathbf{K}_t)) \cdot \mathbf{V}_t, \quad (13)$$

where the attention weight reweighting function $h(\mathbf{Q}_t, \mathbf{K}_t)$ incorporates fairness-guided modulation:

$$h(\mathbf{Q}_t, \mathbf{K}_t) = \frac{\mathbf{Q}_t\mathbf{K}_t^{\top} + \lambda\mathbf{M}_t^{\text{fair}}}{\sqrt{d}}. \quad (14)$$

The fairness-aware modulation term $\mathbf{M}_t^{\text{fair}} \in \mathbb{R}^{(H \cdot W) \times L}$ is constructed as:

$$\mathbf{M}_t^{\text{fair}} = \mathbf{R}_t \odot \mathbf{M}_t^{\text{pos}} - (1 - \mathbf{R}_t) \odot \mathbf{M}_t^{\text{neg}}, \quad (15)$$

with

$$\begin{aligned} \mathbf{M}_t^{\text{pos}} &= \max(\mathbf{Q}_t\mathbf{K}_t^{\top}) - \mathbf{Q}_t\mathbf{K}_t^{\top}, \\ \mathbf{M}_t^{\text{neg}} &= \mathbf{Q}_t\mathbf{K}_t^{\top} - \min(\mathbf{Q}_t\mathbf{K}_t^{\top}). \end{aligned} \quad (16)$$

and the soft similarity mask $\mathbf{R}_t[\mathfrak{q}, k]$ is defined by

$$\mathbf{R}_t[\mathfrak{q}, k] = \begin{cases} \cos(\mathbf{Q}_t[\mathfrak{q}], \mathbf{e}_k), & \text{if } k \in \tau_k, \\ 0, & \text{otherwise.} \end{cases} \quad (17)$$

Here, $\mathfrak{q} \in \{1, \dots, H \cdot W\}$ indexes the spatial query positions, and $k \in \{1, \dots, L\}$ indexes the prompt token positions. $\mathbf{e}_k \in \mathbb{R}^d$ denotes the embedding of the k -th fairness token, and τ_k is the set of key indices corresponding to \mathbf{e}_k . The cosine similarity softly aligns each query to its semantically relevant fairness concept, allowing fine-grained attention modulation. This soft similarity mask \mathbf{R}_t biases the attention logits toward fairness-relevant tokens, ensuring that spatial queries focus more on semantically aligned fairness concepts while suppressing unrelated prompts. Unlike a hard mask, the cosine similarity provides a continuous modulation, preserving the natural attention distribution while improving fine-grained prompt-to-region alignment.

This approach dynamically guides attention toward debiasing-relevant tokens while mitigating interference from irrelevant prompts, thereby enhancing fairness-aware consistency across frames in video generation.

4 Experiments

FairVE: Datasets for Fairness in Frame-Level Video Editing

Data Collection and Fairness Configurations. Following previous studies (Zhang et al. 2024; Jeong et al. 2024), we

construct the *FairVE* dataset consisting of video–text pairs sourced from the DAVIS benchmark and supplemented with high-quality, user-generated videos collected from the web. Rather than relying on artificially designed samples, FairVE reflects naturally occurring social bias in real-world data, ensuring realistic evaluation of fairness-aware VE methods. To better capture and evaluate social bias, we restrict the dataset to scenes containing a single human subject, filtering out clips with animals, vehicles, multiple individuals, or complex backgrounds. The corresponding text prompts are automatically generated using GPT-4 (Feng et al. 2025) to ensure consistency across samples. Each video sequence contains 30 to 60 frames with 512×512 or 640×320 pixels.

In the fairness evaluation protocol, we focus on gender-profession stereotypes observed in SD 1.5 (Kim et al. 2025), as subclass of (Orgad, Kawar, and Belinkov 2023; Chuang et al. 2023). Eight representative professions are selected: CEO, doctor, technician, pilot, teacher, nurse, fashion designer and librarian. Specifically, we combine each profession with gender-specific terms (“male” or “female”) to create 640 prompts (8 professions \times 2 genders \times 40 videos).

Fairness Evaluation We assess the bias correction capability followed by (Kim et al. 2025) and complement it with human evaluations. For each profession specific prompt, FAME is repeated 5 times under different random seeds.

For automatic metrics, We record two metrics: (1) *Correction Count*, the total number of trials in which the edited result shows reduced gender bias compared with the unedited baseline; and (2) *Correction Ratio*, the relative frequency of such bias-reducing outcomes. Higher values indicate more consistent mitigation.

To provide a qualitative perspective, we conduct human evaluation (Friedrich et al. 2023; Li et al. 2025a,b) along three dimensions: *Perceived Bias Correction*, whether the generated portrayal of the profession appears unbiased; *Visual Stability*, the consistency of appearance and motion across frames; and *Semantic Relevance*, the alignment between generated content and the intended meaning of the prompt. Twenty participants rated 640 video-text pairs on a scale from 20 to 100 for each aspect. Averaged scores serve as complementary evidence to the statistical results.

Baselines We compare our model’s fidelity, consistency, and fairness with several SOTA training-free VE methods, including FateZero (Qi et al. 2023), TokenFlow (Geyer et al. 2024), DMT (Yatim et al. 2024), Slicedit (Cohen et al. 2024) and VideoGrain (Yang et al. 2025). Since these baselines do not incorporate fairness mechanisms by design, we adopt a prompt-based mitigation strategy by explicitly injecting bias debiasing terms into their input prompts. We then evaluate both their VE quality and fairness performance using the same metrics, allowing a direct comparison with FAME.

Experimental Results

Fairness Comparison Fairness results are shown in Table 1. From the automatic metrics, professions with strong stereotypes such as *Doctor* and *Nurse* show clear improvements, with high correction ratios and strong bias correction scores. Human evaluation further confirms this: *Bias Correction* ratings exceed 80/100, indicating effective mitigation, while

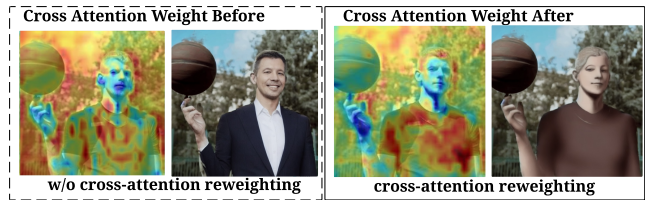


Figure 3: **Cross-Attention Modulation Effect.** Visualization of attention maps corresponding to the token CEO under different ablation settings. The baseline model struggles to separate foreground(human) and background(tree), often overlooking regions related to fairness. Cross-attention reweighting helps adjust areas like outfit to better preserve identity features.

Semantic Relevance remains high, reflecting faithful prompt alignment. *Visual Stability* scores are relatively lower, suggesting temporal consistency still needs improvement. Overall, these results show that our method reduces bias effectively while maintaining semantic fidelity, though motion continuity can be further enhanced.

Video Editing Comparison As shown in Table 2, FAME outperforms all baselines across key CLIP-based metrics, including CLIP-F, CLIP-T (Cong et al. 2024), and TIFA (Hu et al. 2023), demonstrating visual-text alignment, temporal coherence, and image-text fidelity, respectively. Comparing with the results in (Yang et al. 2025; Fan, Bhattad, and Krishna 2024), we re-run the metrics for VideoGrain as a baseline (results are taken directly from (Yang et al. 2025) where our experimental dataset inherits and the comparison is fair). FAME also achieves the lowest warp error, demonstrating better temporal consistency and spatial coherence in the edited sequences. Unlike previous methods, which rely on latent inversion or token warping, FAME incorporates attention modulation, leading to more visually stable and semantically accurate results, especially under attribute-altering prompts. For more visualization results, please refer to our GitHub Pages. The anonymous repository link is available in Appendix ??.

Ablation Study

Cross-Attention Disentanglement To evaluate whether our attention modulation enhances fairness-relevant region separation, we design a simplified version of FAME. Each frame is segmented into a foreground (e.g., man) and a background (e.g., trees) region. We use the prompt “A CEO is spinning ball” to examine cross-attention responses. Without our modulation, the attention weights for the word “CEO” tend to spread into the background, causing semantic interference. As a result, the edited region retains biased visual features, preserving the male outfit. In contrast, with cross-attention reweighting, attention weights become more localized, emphasizing the foreground region while suppressing irrelevant background responses. In that case, the foreground region will be modified more to debiasing content(the outfit of female). This separation is essential for fairness-aware editing, ensuring that debiasing prompt re-

Minor Group	Professions	Automatic		User Study			
		Count	Ratio	Bias Correction↑	Visual Stability↑	Semantic Relevance↑	Overall↑
Female	CEO	9	0.45	70.2	40.2	86.7	65.70
	Doctor	6	0.30	83.7	44.8	89.2	72.57
	Technician	4	0.20	80.8	55.4	88.5	74.90
	Pilot	10	0.50	84.6	48.3	90.1	74.33
Male	Teacher	10	0.50	69.0	59.0	79.6	69.20
	Nurse	2	0.10	88.2	60.8	91.1	80.03
	Fashion designer	9	0.45	71.8	53.1	86.9	70.60
	Librarian	9	0.45	72.9	59.2	87.4	49.83

Table 1: Fairness evaluation across professions and minority groups.

Method	CLIP-based			Other
	CLIP-F ↑	CLIP-T ↑	TIFA ↑	Warp-Err ↓
FateZero	95.75	33.78	48.65	3.08
TokenFlow	96.48	34.59	49.62	2.82
Ground-A-Video	95.17	35.09	/	4.43
DMT	96.34	34.09	/	2.05
VideoGrain	97.18	35.22	60.17	2.21
FAME (Ours)	98.31	35.9	62.2	1.66

Table 2: Quantitative comparison of automatic metrics with FateZero (Qi et al. 2023), TokenFlow (Geyer et al. 2024), Ground-A-Video (Jeong and Ye 2024), DMT (Yatim et al. 2024), VideoGrain (Yang et al. 2025).

lated to protected concepts remain spatially and semantically disentangled from unrelated content. As shown in Figure 3, our module produces a clearer attention focus aligned with the intended semantic region.

Attention Modulation for Fairness Control

We conduct an ablation study to verify the effectiveness of our fairness-guided attention modulation. Specifically, we compare three variants: (1) **Baseline**, which applies text to VE with prompt-guided module; (2) **+ Self-Attn Modulation**, where we introduce fairness alignment using our modulation map R_t ; and (3) **+ Self-Attn + Cross-Attn Modulation**, the full version of our framework.

Quantitative results in Table 3 show that adding self-attention and cross-attention modulation progressively improves CLIP-based metrics, with CLIP-F increasing slightly to 98.30, CLIP-T to 35.80, and TIFA to 61.22, compared to the baseline. Meanwhile, the fairness ratio of male teacher maintain in 0.50, indicating the fairness can be achieved combined with three modules.

Sensitivity Analysis on Text Encoding

To investigate the influence of our fairness-guided prompt encoding strategy, we conduct two controlled sensitivity analyses focusing on the *modulation strength* of the debiasing embedding.

Modulation Strength Sensitivity. We further study the impact of varying the injection strength by introducing a

scaling factor α :

$$g(\mathbf{p}_{\text{fair}}, \mathbf{p}_{\text{tar}}) = \tilde{\mathbf{e}}_{\text{tar}} + \alpha \mathbf{M} \otimes (\mathbf{e}_{\text{fair}} - \tilde{\mathbf{e}}_{\text{tar}}), \quad (18)$$

where $\alpha \in \{0.0, 0.25, 0.5, 1.0\}$.

As illustrated in Appendix Figure 4, smaller values of α result in underwhelming fairness control (e.g., no visible change in target appearance), while excessively large α may distort original semantics. Our method achieves the best trade-off when $\alpha = 0.5$, offering both fairness alignment and semantic stability.

Ablation Settings	VE Quality			Fairness
	CLIP-F ↑	CLIP-T ↑	TIFA ↑	Ratio
+P	95.70	33.99	49.6	/
+P +S	98.10	35.10	60.37	0.50
+P +S +C	98.30	35.80	61.22	0.50

Table 3: Ablation study of key modules. P: *Prompt-guided module*; S: *Self-attention module*; C: *Cross-attention module*. Modules are added cumulatively from top to bottom.

5 Conclusion

In this paper, we present a training-free framework FAME for fairness-aware VE that addresses the limitations of existing diffusion-based models in handling fairness-sensitive prompts. By introducing soft debiasing prompt encoding and fairness-guided modulation in both self-attention and cross-attention layers, FAME ensures improved alignment between textual attributes and visual regions while preserving temporal coherence. To support systematic evaluation, we construct FairVE, the first benchmark dataset tailored for assessing fairness in VE tasks, encompassing diverse gender–profession combinations. Extensive experiments, including automatic metrics and structured human evaluations, show that FAME outperforms state-of-the-art zero-shot baselines in semantic fidelity, visual consistency, and bias mitigation. Because FAME works entirely at the inference time, it avoids expensive retraining yet still improves fairness and stability. We will extend this strategy for broader fairness-aware VE research.

References

- Azam, B.; and Akhtar, N. 2025. Plug-and-Play Interpretable Responsible Text-to-Image Generation via Dual-Space Multi-facet Concept Control. In *CVPR*.
- Birhane, A.; Prabhu, V. U.; and Kahembwe, E. 2021. Multimodal Datasets: Misogyny, Pornography, and Malignant Stereotypes. *arXiv*.
- Brack, M.; Friedrich, F.; Hintersdorf, D.; Struppek, L.; Schramowski, P.; and Kersting, K. 2023. SEGA: Instructing Text-to-Image Models using Semantic Guidance. *NeurIPS*.
- Chefer, H.; Alaluf, Y.; Vinker, Y.; Wolf, L.; and Cohen-Or, D. 2024. Attend-and-Excite: Attention-based Semantic Guidance for Text-to-Image Diffusion Models. *TOG*.
- Cheng, Y.; Li, L.; Xu, Y.; Li, X.; Yang, Z.; Wang, W.; and Yang, Y. 2023. Segment and Track Anything. *arXiv*.
- Cho, J.; Zala, A.; and Bansal, M. 2023. DALL-EVAL: Probing the Reasoning Skills and Social Biases of Text-to-Image Generation Models. In *ICCV*.
- Chuang, C.-Y.; Jampani, V.; Li, Y.; Torralba, A.; and Jegelka, S. 2023. Debiasing Vision-Language Models via Biased Prompts. *arXiv*.
- Cohen, N.; Kulikov, V.; Kleiner, M.; Huberman-Spiegelglas, I.; and Michaeli, T. 2024. Slicedit: Zero-Shot Video Editing with Text-to-Image Diffusion Models using Spatio-Temporal Slices. *ICML*.
- Cong, Y.; Xu, M.; Simon, C.; Chen, S.; Ren, J.; Xie, Y.; Perez-Rua, J.-M.; Rosenhahn, B.; Xiang, T.; and He, S. 2024. Flatten: Optical Flow-guided Attention for Consistent Text-to-Video Editing. *ICLR*.
- Dewan, S.; Zawat, R.; Saxena, P.; Chang, Y.; Luo, A.; and Bisk, Y. 2024. Diffusion PID: Interpreting Diffusion via Partial Information Decomposition. *NeurIPS*.
- Fan, X.; Bhattad, A.; and Krishna, R. 2024. Videoshop: Localized Semantic Video Editing with Noise-Extrapolated Diffusion Inversion. *ECCV*.
- Feng, R.; Weng, W.; Wang, Y.; Yuan, Y.; Bao, J.; Luo, C.; Chen, Z.; and Guo, B. 2024. Ccredit: Creative and Controllable Video Editing via Diffusion Models. *CVPR*.
- Feng, Y.; Gao, S.; Bao, Y.; Wang, X.; Han, S.; Zhang, J.; Zhang, B.; and Yao, A. 2025. WAVE: Warping Ddim Inversion Features for Zero-Shot Text-to-Video Editing. *ECCV*.
- Friedrich, F.; Brack, M.; Struppek, L.; Hintersdorf, D.; Schramowski, P.; Luccioni, S.; and Kersting, K. 2023. Fair Diffusion: Instructing Text-to-Image Generation Models on Fairness. *arXiv*.
- Gandikota, R.; Orgad, H.; Belinkov, Y.; Materzyńska, J.; and Bau, D. 2024. Unified Concept Editing in Diffusion Models. *Winter Conference on Applications of Computer Vision*.
- Geyer, M.; Bar-Tal, O.; Bagon, S.; and Dekel, T. 2024. Tokenflow: Consistent Diffusion Features for Consistent Video Editing. *ICLR*.
- Hertz, A.; Mokady, R.; Tenenbaum, J.; Aberman, K.; Pritch, Y.; and Cohen-Or, D. 2023. Prompt-to-Prompt Image Editing with Cross Attention Control. *ICLR*.
- Ho, J.; and Salimans, T. 2022. Classifier-free Diffusion Guidance. *NeurIPS*.
- Ho, J.; Salimans, T.; Gritsenko, A.; Chan, W.; Norouzi, M.; and Fleet, D. J. 2022. Video Diffusion Models. *NeurIPS*.
- Hu, Y.; Liu, B.; Kasai, J.; Wang, Y.; Ostendorf, M.; Krishna, R.; and Smith, N. A. 2023. TIFA: Accurate and Interpretable Text-to-Image Faithfulness Evaluation with Question Answering. In *CVPR*.
- Huang, H.; Jin, X.; Miao, J.; and Wu, Y. 2025. Implicit Bias Injection Attacks against Text-to-Image Diffusion Models. In *CVPR*.
- Jeong, H.; Chang, J.; Park, G. Y.; and Ye, J. C. 2024. Dreammotion: Space-Time Self-Similar Score Distillation for Zero-Shot Video Editing. *ECCV*.
- Jeong, H.; and Ye, J. C. 2024. Ground-a-video: Zero-Shot Grounded Video Editing using Text-to-Image Diffusion Models. *ICLR*.
- Jung, H.; Jang, T.; and Wang, X. 2024. A Unified Debiasing Approach for Vision-Language Models Across Modalities and Tasks. *NeurIPS*.
- Jung, S.; Oesterling, A.; Verdun, C. M.; Vithana, S.; Moon, T.; and Calmon, F. P. 2025. Multi-Group Proportional Representations for Text-to-Image Models. In *CVPR*.
- Kahatapitiya, K.; Karjauv, A.; Abati, D.; Porikli, F.; Asano, Y. M.; and Habibian, A. 2025. Object-Centric Diffusion for Efficient Video Editing. *ECCV*.
- Kara, O.; Kurtkaya, B.; Yesiltepe, H.; Rehg, J. M.; and Yanardag, P. 2024. Rave: Randomized Noise Shuffling for Fast and Consistent Video Editing with Diffusion Models. *CVPR*.
- Karmann, M.; and Urfalioglu, O. 2025. Repurposing Stable Diffusion Attention for Training-free Unsupervised Interactive Segmentation. In *CVPR*.
- Kim, E.; Kim, S.; Park, M.; Entezari, R.; and Yoon, S. 2025. Rethinking Training for De-biasing Text-to-Image Generation: Unlocking the Potential of Stable Diffusion. *CVPR*.
- Lee, B. H.; Lim, S.; and Chun, S. Y. 2025. Localized Concept Erasure for Text-to-Image Diffusion Models using Training-Free Gated Low-Rank Adaptation. In *CVPR*.
- Li, H.; Shen, C.; Torr, P.; Tresp, V.; and Gu, J. 2024a. Self-Discovering Interpretable Diffusion Latent Directions for Responsible Text-to-Image Generation. In *CVPR*.
- Li, J.; Hu, L.; Zhang, J.; Zheng, T.; Zhang, H.; and Wang, D. 2025a. Fair Text-to-Image Diffusion via Fair Mapping. In *Association for the Advancement of Artificial Intelligence*.
- Li, L.; Shi, Z.; Hu, X.; Dong, B.; Qin, Y.; Liu, X.; Sheng, L.; and Shao, J. 2025b. T2ISafety: Benchmark for Assessing Fairness, Toxicity, and Privacy in Image Generation. *arXiv*.
- Li, M.; Li, Y.; Yang, T.; Liu, Y.; Yue, D.; Lin, Z.; and Xu, D. 2024b. A Video is Worth 256 Bases: Spatial-Temporal Expectation-Maximization Inversion for Zero-Shot Video Editing. *CVPR*.
- Li, X.; Ma, C.; Yang, X.; and Yang, M.-H. 2024c. VidTome: Video Token Merging for Zero-Shot Video Editing. *CVPR*.

- Li, Z.; Chen, D.; Fan, M.; Chen, C.; Li, Y.; Wang, Y.; and Zhou, W. 2025c. Responsible Diffusion Models via Constraining Text Embeddings Within Safe Regions. In *WWW*.
- Liu, B.; Wang, C.; Cao, T.; Jia, K.; and Huang, J. 2024a. Towards Understanding Cross and Self-attention in Stable Diffusion for Text-guided Image Editing. In *CVPR*.
- Liu, S.; Zhang, Y.; Li, W.; Lin, Z.; and Jia, J. 2024b. Video-p2p: Video Editing with Cross-Attention Control. In *CVPR*.
- Mokady, R.; Hertz, A.; Aberman, K.; Pritch, Y.; and Cohen-Or, D. 2023. Null-text Inversion for Editing Real Images using Guided Diffusion Models. In *CVPR*.
- Orgad, H.; Kawar, B.; and Belinkov, Y. 2023. Editing Implicit Assumptions in Text-to-Image Diffusion Models. In *ICCV*.
- Park, J.; Lee, J.; Chung, C.; Lee, J.; Choo, J.; and Gu, J. 2025. Fair Generation without Unfair Distortions: Debiasing Text-to-Image Generation with Entanglement-Free Attention. *arXiv*.
- Qi, C.; Cun, X.; Zhang, Y.; Lei, C.; Wang, X.; Shan, Y.; and Chen, Q. 2023. Fatezero: Fusing Attentions for Zero-shot Text-based Video Editing. *ICCV*.
- Radford, A.; Kim, J. W.; Hallacy, C.; Ramesh, A.; Goh, G.; Agarwal, S.; Sastry, G.; Askell, A.; Mishkin, P.; Clark, J.; et al. 2021. Learning Transferable Visual Models from Natural Language Supervision. In *ICML*.
- Ramesh, A.; Pavlov, M.; Goh, G.; Gray, S.; Voss, C.; Radford, A.; Chen, M.; and Sutskever, I. 2021. Zero-shot Text-to-Image Generation. In *ICML*.
- Rombach, R.; Blattmann, A.; Lorenz, D.; Esser, P.; and Ommer, B. 2022. High-resolution Image Synthesis with Latent Diffusion Models. In *CVPR*.
- Ross, C.; Katz, B.; and Barbu, A. 2021. Measuring Social Biases in Grounded Vision and Language Embeddings. *NAACL*.
- Shen, X.; Du, C.; Pang, T.; Lin, M.; Wong, Y.; and Kankanhalli, M. 2024. Finetuning Text-to-Image Diffusion Models for Fairness. *ICLR*.
- Shi, Y.; Li, C.; Wang, Y.; Zhao, Y.; Pang, A.; Yang, S.; Yu, J.; and Ren, K. 2025. Dissecting and Mitigating Diffusion Bias via Mechanistic Interpretability. In *CVPR*.
- Singer, U.; Polyak, A.; Hayes, T.; Yin, X.; An, J.; Zhang, S.; Hu, Q.; Yang, H.; Ashual, O.; Gafni, O.; et al. 2022. Make-a-Video: Text-to-Video Generation without Text-to-Video Data. *arXiv*.
- Song, J.; Meng, C.; and Ermon, S. 2021. Denoising Diffusion Implicit Models. *ICLR*.
- Teed, Z.; and Deng, J. 2020. Raft: Recurrent All-Pairs Field Transforms for Optical Flow. In *ECCV*.
- Teo, C. T.; Abdollahzadeh, M.; Ma, X.; and Cheung, N.-m. 2024. Fairqueue: Rethinking Prompt Learning for Fair Text-to-Image Generation. *NeurIPS*.
- Wang, J.; Ma, Y.; Guo, J.; Xiao, Y.; Huang, G.; and Li, X. 2024. Cove: Unleashing the Diffusion Feature Correspondence for Consistent Video Editing. *NeurIPS*.
- Wu, J. Z.; Ge, Y.; Wang, X.; Lei, S. W.; Gu, Y.; Shi, Y.; Hsu, W.; Shan, Y.; Qie, X.; and Shou, M. Z. 2023a. Tune-a-Video: One-Shot Tuning of Image Diffusion Models for Text-to-Video Generation. In *CVPR*.
- Wu, J. Z.; Ge, Y.; Wang, X.; Lei, W.; Gu, Y.; Shi, Y.; Hsu, W.; Shan, Y.; Qie, X.; and Shou, M. Z. 2023b. Tune-a-Video: One-Shot Tuning of Image Diffusion Models for Text-to-Video Generation. *ICCV*.
- Yang, X.; Zhu, L.; Fan, H.; and Yang, Y. 2025. Videograin: Modulating Space-Time Attention for Multi-Grained Video Editing. *ICLR*.
- Yatim, D.; Fridman, R.; Bar-Tal, O.; Kasten, Y.; and Dekel, T. 2024. Space-time Diffusion Features for Zero-Shot Text-driven Motion Transfer. In *CVPR*.
- Zhang, G.; Zhang, T.; Niu, G.; Tan, Z.; Bai, Y.; and Yang, Q. 2024. CAMEL: Causal Motion Enhancement Tailored for Lifting Text-Driven Video Editing. *CVPR*.
- Zhang, L.; Rao, A.; and Agrawala, M. 2023. Adding Conditional Control to Text-to-Image Diffusion Models. In *ICCV*.
- Zhong, X.; Huang, X.; Yang, X.; Lin, G.; and Wu, Q. 2025. Deco: Decoupled Human-Centered Diffusion Video Editing with Motion Consistency. *ECCV*.
- Zhou, J.; Gao, J.; Zhao, X.; Yao, X.; and Wei, X. 2024. Association of Objects May Engender Stereotypes: Mitigating Association-Engendered Stereotypes in Text-to-Image Generation. *NeurIPS*.

6 Appendix

Existing literature on Fairness in T2I methods

Prior work on fair T2I mostly falls into three camps: adding semantic guidance during diffusion optimization (Dewan et al. 2024; Shen et al. 2024; Jung et al. 2025), injecting debiasing embeddings into the latent space (Huang et al. 2025; Azam and Akhtar 2025; Li et al. 2025c), or applying classifier-guided noise control (Brack et al. 2023; Kim et al. 2025). Lightweight alternatives modify attention maps (Gandikota et al. 2024; Teo et al. 2024; Zhou et al. 2024; Park et al. 2025) or adjust the bottleneck representations in the U-Net (Li et al. 2024a; Shi et al. 2025), avoiding full model retraining.

Implementation Details

VE Evaluation Metrics To demonstrate that our model effectively preserves VE capabilities, we adopt a suite of established CLIP similarity metrics (Radford et al. 2021) that capture both edit fidelity and temporal consistency. We primarily focus on CLIP-based metrics to measure semantic alignment and structural coherence. Specifically, we employ CLIP-T, which calculates the average cosine similarity between the input text prompt and all generated video frames using CLIP embeddings, thereby reflecting how well the output video aligns with the intended prompt semantics. CLIP-F measures the average cosine similarity between consecutive video frames, serving as an indicator of temporal coherence within the generated sequence. TIFA score evaluates semantic alignment between the target image and the edited video frames. Additionally, Warp-Err quantifies the pixel-level deviation by warping each edited frame based on the optical flow of the source video using *RAFT-Large* (Teed and Deng 2020), thereby evaluating motion consistency.

Experimental Settings We build our framework upon SD 1.5¹, utilizing its released pre-trained weights along with the DDIM scheduler (Song, Meng, and Ermon 2021) with 50 steps for inverse to acquire attention maps. Each video-text pair is represented as the tuple (source video, instruction, SAM masks, ControlNet annotators). We employ SAM-tracking (Cheng et al. 2023) based masks to perform object-level clustering, enabling fine-grained edge segmentation. To support controllable image-level editing, we integrate several ControlNet annotators (Zhang, Rao, and Agrawala 2023), including DW-Pose, Depth-Zoe, Depth-MiDaS, and OpenPose (totaling approximately 4 GB). We retain the default `guidance_scale` parameter to control the influence of the prompt on the editing outcome. Additionally, we enable Prompt-to-Prompt (PnP) (Hertz et al. 2023) editing to modulate spatial or semantic regions across frames. All experiments are conducted on a single NVIDIA Tesla H100 GPU.

Additional Results

Figure 4 verify the necessity of the importance of balanced modulation strength for fairness-aware prompt design in T2I based training-free VE models.

¹<https://huggingface.co/stable-diffusion-v1-5/stable-diffusion-v1-5>

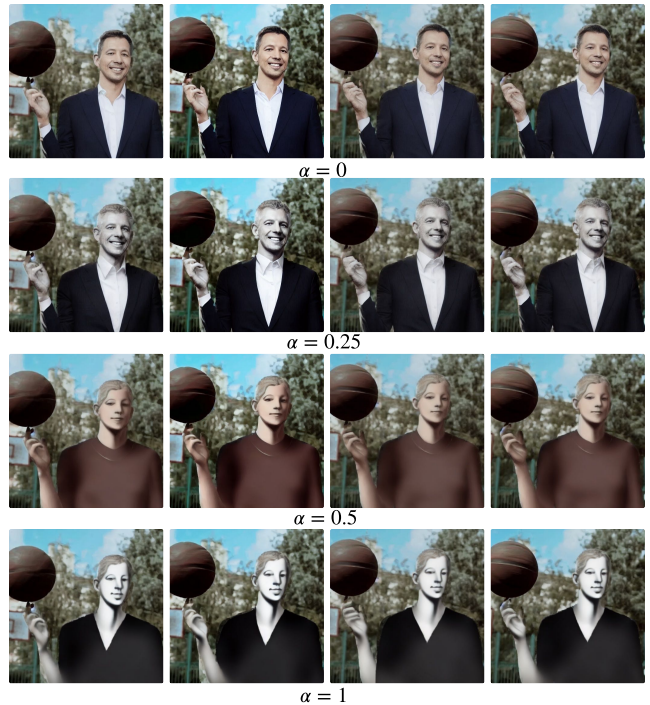


Figure 4: Comparison of different prompt injection methods. Direct addition leads to semantic confusion, while our masked fusion retains structure and enhances fairness controllability.

Figure 5 shows the full test pipeline and results for the Prompt Responsiveness Test mentioned in Section 3.

Pseudo Algorithm Code. Our full inference procedure is composed of three core modules, shown in Algorithm 1, Algorithm 2 and Algorithm 3. Algorithm 1 describes the fairness-aware text embedding procedure, which softly fuses debiasing attribute tokens into the original prompt embedding to retain semantic structure while introducing fairness control. Algorithm 2 defines the fairness-aware self-attention modulation that enhances intra-region coherence by amplifying attention within fairness-relevant areas and suppressing unrelated interactions. Algorithm 3 introduces the fairness-aware cross-attention mechanism, where alignment between prompt tokens and visual regions is refined using a similarity-based attention mask.



Figure 5: **Prompt Responsiveness Test.** We evaluate three training-free VE models, including FateZero, TokenFlow, and VideoGrain, on a single example P_{ref} = "A man is playing tennis" to assess their responsiveness to debiasing prompt. The top row shows the input reference frames. Rows 2–4 display results using different prompts on several baselines, including FateZero (Qi et al. 2023), TokenFlow (Geyer et al. 2024), and VideoGrain (Yang et al. 2025), while the 5th row shows the results with the original editing prompt P_{tar} = "A teacher is playing tennis" by our FAME. In rows 2–4, the left column shows the editing performance with the original prompt, and the right column shows the editing performance guided by the directly injected debiasing prompt P_{tar} = "A male teacher is playing tennis" as the debiasing prompt. In the last row, our FAME can generate the female version (left column) and the debiased male content (right column). In the 2nd and 3rd rows, FateZero and TokenFlow exhibit a mismatch between the debiasing prompt and the visual semantics, indicating degraded video fidelity. In the 4th row, VideoGrain shows that directly injecting debiasing prompts often leads to semantic degradation in generated frames. This suggests that fairness-sensitive prompts may disrupt the alignment between the prompt and visual output. In the last row, our FAME can generate different gender-profession content even with the original prompt.

Algorithm 1: Soft Debiasing Prompt Encoding via Position-Aware Fusion

Require: Target prompt \mathbf{p}_{tar} , fairness prompt \mathbf{p}_{fair} , pre-trained text encoder ϕ
Ensure: Debaised embedding matrix $\tilde{\mathbf{e}} \in \mathbb{R}^{L \times d}$

- 1: $\mathbf{e}_{\text{tar}} \leftarrow \phi(\mathbf{p}_{\text{tar}})$ // Token embeddings of target prompt
- 2: $\mathbf{e}_{\text{fair}} \leftarrow \phi(\mathbf{p}_{\text{fair}})$ // Token embeddings of fairness prompt
- 3: $\mathbf{M} \leftarrow \text{GENERATESOFTMASK}(\mathbf{e}_{\text{tar}}, \mathbf{e}_{\text{fair}})$ // Soft mask: $\mathbf{M} \in [0, 1]^{L \times d}$
- 4: $\tilde{\mathbf{e}} \leftarrow \mathbf{e}_{\text{tar}} + \mathbf{M} \otimes (\mathbf{e}_{\text{fair}} - \mathbf{e}_{\text{tar}})$ // Soft injection
- 5: **return** $\tilde{\mathbf{e}}$

Algorithm 2: Self-attention Manipulation

Require: Latent tensor $\mathbf{z}_t \in \mathbb{R}^{h \times w \times \ell \times c}$, projections $W_{\mathbf{Q}}, W_{\mathbf{K}}, W_{\mathbf{V}}$, coefficients λ, μ , temperature τ
Ensure: Attention output $\mathbf{A} \in \mathbb{R}^{(h \cdot w) \times \ell \times d}$

- 1: $\mathbf{z}' \leftarrow \varphi(\mathbf{z}_t)$ // Flatten spatial dims to $(h \cdot w) \times \ell \times c$
- 2: $\mathbf{Q}, \mathbf{K}, \mathbf{V} \leftarrow W_{\mathbf{Q}}\mathbf{z}', W_{\mathbf{K}}\mathbf{z}', W_{\mathbf{V}}\mathbf{z}'$ // Project to attention space
- 3: $\mathbf{A}_{\text{raw}} \leftarrow \mathbf{Q}\mathbf{K}^{\top}$ // Raw attention scores
- 4: Compute $\mathbf{M}^{\text{pos}}, \mathbf{M}^{\text{neg}}$ from \mathbf{A}_{raw}
- 5: Compute region mask \mathbf{R} // 1 if same region, else 0
- 6: $\mathbf{M}^{\text{fair}} \leftarrow \mathbf{R} \odot \mathbf{M}^{\text{pos}} - (1 - \mathbf{R}) \odot \mathbf{M}^{\text{neg}}$
- 7: Compute per-position feature mean: $\mathbf{f}_{\mathbf{q}} = \frac{1}{\ell} \sum_{t=1}^{\ell} \mathbf{z}_t[\mathbf{q}]$
- 8: Compute similarity mask: $\mathbf{S}[\mathbf{q}_1, \mathbf{q}_2] = \exp(-\|\mathbf{f}_{\mathbf{q}_1} - \mathbf{f}_{\mathbf{q}_2}\|^2 / \tau^2)$
- 9: $g(\mathbf{Q}, \mathbf{K}) \leftarrow (\mathbf{A}_{\text{raw}} + \lambda \mathbf{M}^{\text{fair}} + \mu \mathbf{S}) / \sqrt{d}$
- 10: $\mathbf{A} \leftarrow \text{softmax}(g(\mathbf{Q}, \mathbf{K})) \cdot \mathbf{V}$ // Final output
- 11: **return** \mathbf{A}

Algorithm 3: Cross-attention Reweighting

Require: $\mathbf{Q}_t, \mathbf{K}_t, \mathbf{V}_t$, fairness token set $\{\mathbf{e}_k\}$, token groups $\{\tau_k\}$, coefficient λ
Ensure: Cross-attention output \mathbf{A}_t

- 1: $\mathbf{A}_{\text{raw}} \leftarrow \mathbf{Q}_t \mathbf{K}_t^{\top}$ // Raw attention matrix
- 2: Compute $\mathbf{M}_t^{\text{pos}}, \mathbf{M}_t^{\text{neg}}$ from \mathbf{A}_{raw}
- 3: **for** each spatial query index \mathbf{q} **do**
- 4: **for** each prompt token index k **do**
- 5: **if** $k \in \tau_k$ **then**
- 6: $\mathbf{R}_t[\mathbf{q}, k] \leftarrow \cos(\mathbf{Q}_t[\mathbf{q}], \mathbf{e}_k)$ // Fairness match
- 7: **else**
- 8: $\mathbf{R}_t[\mathbf{q}, k] \leftarrow 0$
- 9: **end if**
- 10: **end for**
- 11: **end for**
- 12: $\mathbf{M}_t^{\text{fair}} \leftarrow \mathbf{R}_t \odot \mathbf{M}_t^{\text{pos}} - (1 - \mathbf{R}_t) \odot \mathbf{M}_t^{\text{neg}}$
- 13: $h(\mathbf{Q}_t, \mathbf{K}_t) \leftarrow (\mathbf{A}_{\text{raw}} + \lambda \mathbf{M}_t^{\text{fair}}) / \sqrt{d}$
- 14: $\mathbf{A}_t \leftarrow \text{softmax}(h(\mathbf{Q}_t, \mathbf{K}_t)) \cdot \mathbf{V}_t$ // Cross-attention output
- 15: **return** \mathbf{A}_t
